Progress In Electromagnetics Research Letters, Vol. 67, 19–24, 2017

A Second Order Decoupling Design Using a Resonator and an Interdigital Capacitor for a MIMO Antenna Pair

Ziyang Wang, Luyu Zhao*, Aobo Chen, and Yingzeng Yin

Abstract—In this paper, a second-order decoupling design using a resonator and an interdigital capacitor is proposed for an MIMO antenna pair in mobile terminals. The proposed antenna pair consists of an interdigital capacitor and an open loop resonator. By properly combining the responses of the resonator and interdigital capacitor, a second-order decoupling performance can be achieved. Meanwhile, isolation between the two antennas is increased by at least 15 dB within the frequency band of interest, from −5 dB to −20 dB. Moreover, the decoupled antenna pair maintains good impedance matching performance from 2.4 GHz to 2.5 GHz. The proposed decoupled antenna pair and its coupled counterpart have been fabricated and measured. The measured results agree with the simulation ones. The proposed MIMO antenna pair is an eligible candidate for Wi-Fi MIMO applications in the 2.4 GHz band.

1. INTRODUCTION

In a next generation wireless communication system, the demand for high rate and more reliable data transmission is dramatically increasing. Multiple-input multiple-output (MIMO) [1] systems have been widely deployed and seem to be the most promising technology for further boosting data throughput. However, in real-world systems, antennas must be closely packed. The mutual coupling and correlation between antennas are therefore inevitably high.

Currently, various methods have been used to decrease antenna mutual coupling [2–11]. In [2], a parasitic ring resonator with half wavelength is used. In [3–5], neutralization lines are introduced to create a second path of current, while the radiation patterns of the antennas with the line will be affected. In [6], a small branch is introduced to improve the antenna to antenna isolation with a fractional bandwidth of 12.4%. Eigen-mode has also been used in MIMO antenna decoupling designs, as reported in [7–9], and the orthogonality of the modes is utilized. Artificial metamaterial structures as a good approach are used in [9–11]. Electromagnetic band gap (EBG) structures [10–12] are used to suppress surface wave propagation for decreasing the mutual coupling in a wide band. Split ring resonator (SRRs) units with negative magnetic are introduced to reduce mutual coupling in a high-profile MIMO antenna design [13]. Defected ground structure (DGS) as an effective artificial unit is etched on the ground as shown in [14]. Coupled resonator decoupling network (CRDN) is reported in [15–20], which can realize a high-order isolation response for wideband applications.

In this letter, a new decoupling method for MIMO antennas is presented. An interdigital capacitor and an open loop resonator are introduced between two monopole antennas to decrease their mutual coupling. By combining the response of the resonator and interdigital capacitor, a second order decoupling performance with wide bandwidth can be obtained. The proposed antenna pair is fabricated and measured. The detailed design process and measured results for the proposed antennas are shown in the following sections.

Received 23 January 2017, Accepted 17 March 2017, Scheduled 30 March 2017

* Corresponding author: Luyu Zhao (lyzhao@xidian.edu.cn).

The authors are with the Key Laboratory of Science and Technology on Antennas and Microwaves, Xidian University, Xi'an, Shaanxi 710071, People's Republic of China.

2. ANTENNA CONFIGURATION

The evolution of the proposed decoupling antenna is shown in Fig. 1. As shown in Fig. 1, ant 1 design is a monopole antenna pair with poor isolation. The pair of monopole antennas is printed on the top layer of an FR4 substrate with a dielectric constant of 4.4, a loss tangent of 0.02, and a thickness of 1.6 mm. A rectangular ground plane is printed on the bottom layer of the substrate. In ant 2 design, an open loop resonator is introduced between the coupled antenna pair, but the impedance and isolation performances are not ideal. Therefore, an interdigital capacitor is connected between the coupled antenna pair as shown in ant 3. By properly combining the responses of the two resonator structures, a second-order isolation performance is obtained, and the impedance matching becomes good. The geometry of the decoupled antenna pair is shown in Fig. 2. With the help of the high-frequency structure simulator, the sizes of the proposed antennas are optimized and shown in Table 1.

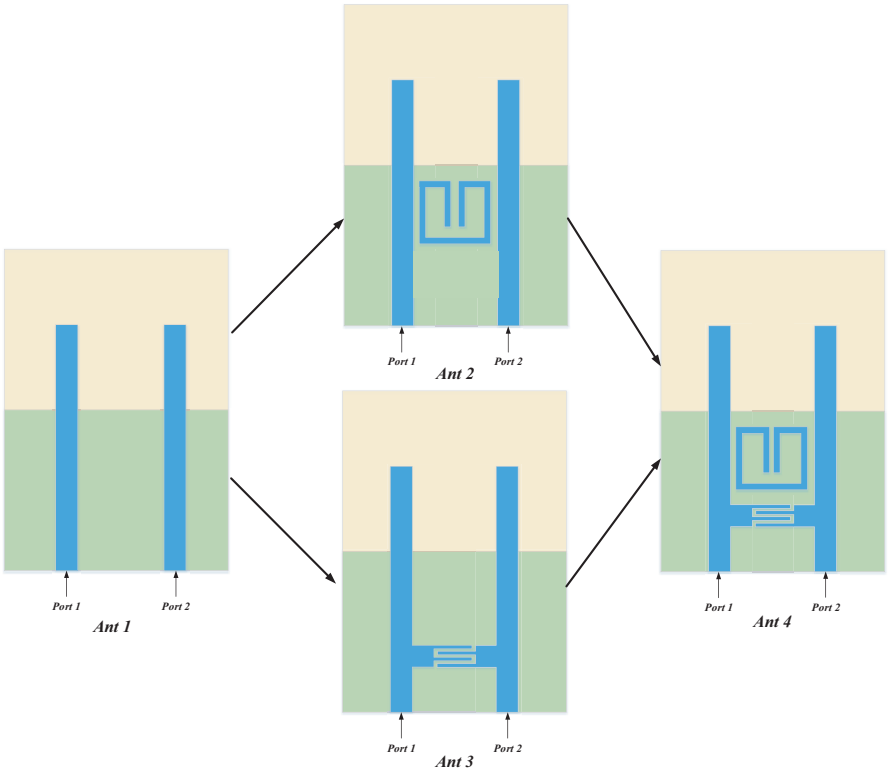

Figure 1. The evolution for the proposed MIMO antenna pair.

Table 1. Detail dimensions of the proposed antenna (unit: mm).

Parameters	Values (mm)	Parameters	Values (mm)	Parameters	Values (mm)
Wg	72	$W1$	2.9	$L7$	3
Lg	40	$W2$	2.8	$L8$	5.5
W	3	$L3$	11.2	Ls	27
$Lsub$	90	$L4$	22	$W3$	0.5
$L1$	4.3	$L5$	5.45	$W4$	0.3
$L2$	54.6	$L6$	15	Lc	12

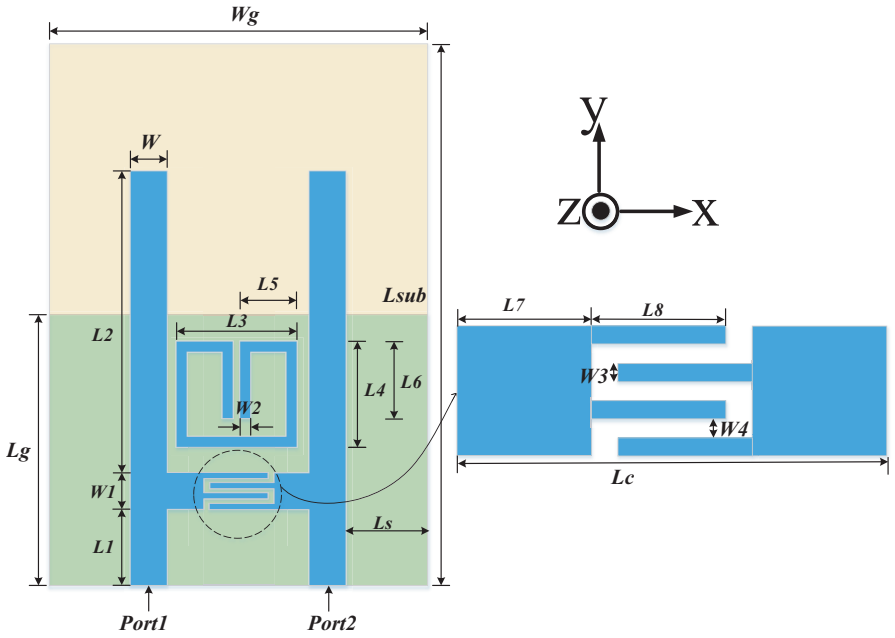

Figure 2. Geometry of the proposed MIMO antenna pair.

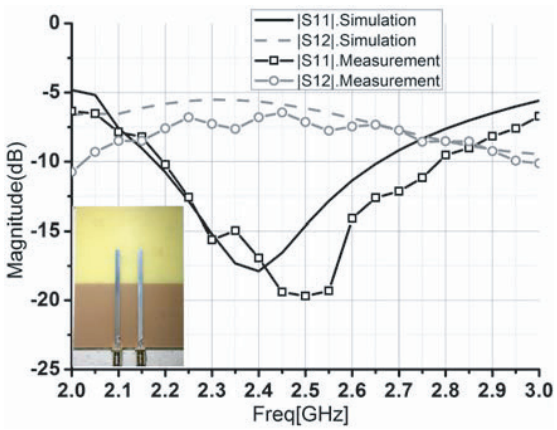

Figure 3. Photograph and S-parameters for the coupled antennas.

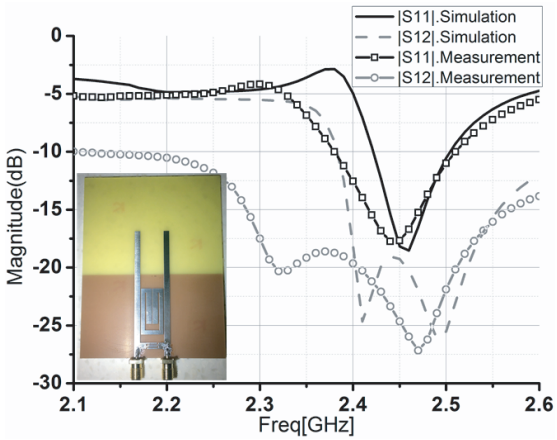

Figure 4. Photograph and S-parameters for the decoupled antennas.

3. MEASUREMENT RESULTS AND DISCUSSION

As shown in Fig. 3 and Fig. 4, the high-frequency structure simulator HFSS15 is used to analyze the coupled and decoupled antennas, and then the prototypes of the coupled and decoupled antennas are fabricated based on the dimensions shown in Table 1. The Keysight E5080A vector network analyser is used to measure the S-parameter performance. Fig. 3 shows the simulated and measured results of the S-parameters for the coupled antenna pair. The impedance matching bandwidth is 590 MHz from 2.2 to 2.79 GHz with $|S_{11}|$ less than -10 dB, while the isolation of the coupled antenna pair is about -6 dB in the same band, which is very poor for MIMO transmission and reception. In Fig. 4, the simulated and measured S parameters for the decoupled antenna pair are superposed. The isolation performance at the WLAN band exceeds 20 dB, which demonstrates that the open loop resonator and interdigital capacitor are effective. Meanwhile, the impedance matching is well maintained simultaneously in the

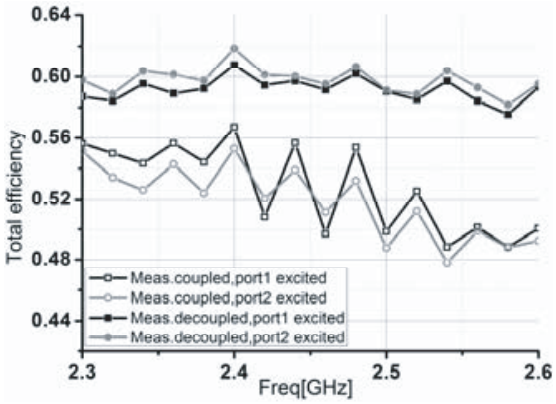

Figure 5. Measured total efficiencies for the coupled and decoupled antenna pair.

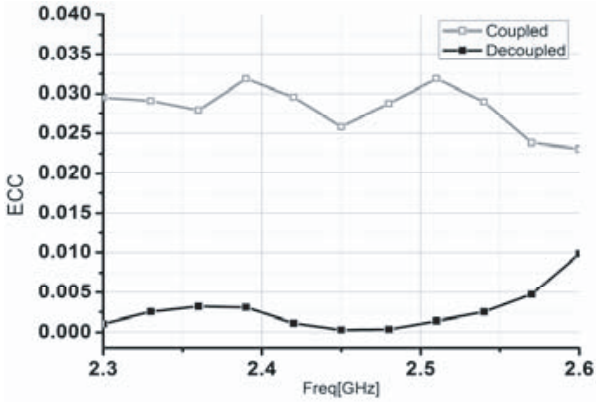

Figure 6. ECC for the coupled and decoupled antennas.

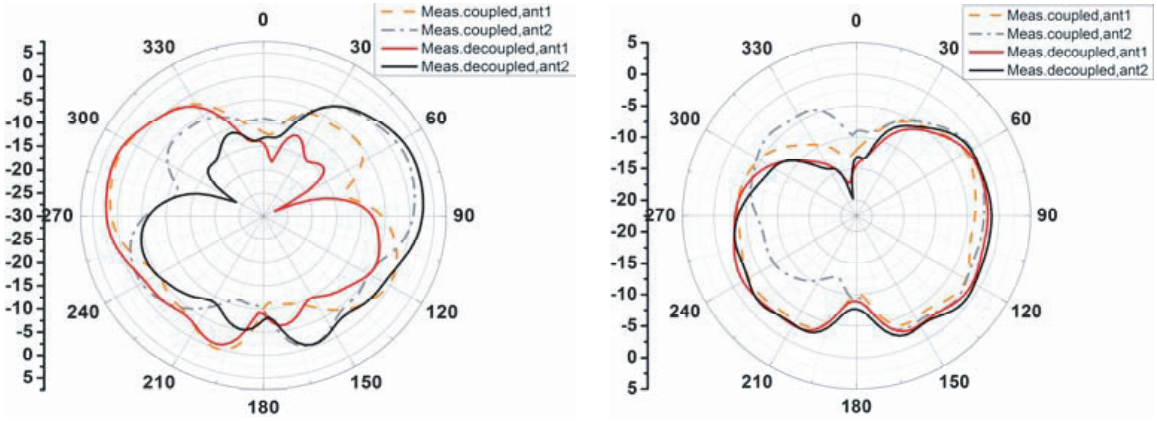

Figure 7. Measured radiation patterns of each antennas of the coupled and decoupled antenna pairs in (a) x-z plane, and (b) y-z plane. (a) xoz plane. (b) yoz plane.

desired band. The antenna pair's radiation performances are evaluated in a SATIMO SG-24 near field scanner. In Fig. 5, the measured total efficiency for the coupled and decoupled antenna pairs are presented. The total efficiency considering both radiation efficiency and reflection efficiency for the decoupled antenna pair are about 60%, while the total efficiencies for the coupled antenna pair are about 53%. Moreover, the envelope correlation coefficient (ECC) as an important figure of merit is also calculated from measure complex patterns. The calculation can be conducted using Equation (1).

$$\rho_e = \frac{\left| \iint\limits_{4\pi} [\vec{E}_1(\theta,\phi) \cdot \vec{E}_2(\theta,\phi)] d\Omega \right|^2}{\iint\limits_{4\pi} |\vec{E}_1(\theta,\phi)|^2 d\Omega \iint\limits_{4\pi} |\vec{E}_2(\theta,\phi)|^2 d\Omega} \tag{1}$$

$$\vec{E}_1(\theta,\phi) \cdot \vec{E}_2(\theta,\phi) = \vec{E}_{\theta 1}(\theta,\phi)\vec{E}^*_{\theta 2}(\theta,\phi) + \vec{E}_{\phi 1}(\theta,\phi)\vec{E}^*_{\phi 2}(\theta,\phi) \tag{2}$$

where $\vec{E}_1(\theta,\phi)$ is the electric field radiated by antenna 1 with antenna 2 terminated by a matched load. Similarly, $\vec{E}_2(\theta,\phi)$ is generated by antenna 2 with antenna 1 terminated by a matched load. Subscript θ means the theta component of the radiated electric field while subscript ϕ indicates the phi component of the radiated electric field.

The ECC curves for the coupled and decoupled antenna pairs are shown in Fig. 6. And the values of the ECC for decoupled antennas are about 0.005 in the desire band. Therefore, the decoupled antennas can be a good candidate for any MIMO systems.

To further study the performance for the decoupled antennas, the radiation patterns are investigated. The measured radiation patterns of the primary polarization for coupled and decoupled antennas (in x-z plane, y-z plane) at resonant frequency 2.45 GHz are shown in Fig. 7.

4. CONCLUSION

In this letter, an MIMO antenna pair with a second-order decoupling performance is proposed. The prototypes of the coupled and decoupled antenna pairs are fabricated and measured. Due to the introduction of an open loop structure and an interdigital capacitor, the isolation performance for the decoupled antenna pair decreases 14 dB compared to the coupled antenna pair in 2.4 GHz band. Moreover, the efficiencies, ECCs, and the radiation patterns for the proposed decoupled antenna pair are satisfactory. Therefore, the designed antenna pair is very suitable for Wi-Fi MIMO applications.

REFERENCES

1. Jensen, M. A. and J. W. Wallace, "A review of antennas and propagation for MIMO wireless communications," *IEEE Trans. Antennas Propag.*, Vol. 52, No. 11, 2810–2824, Nov. 2004.
2. Lee, C. H., S. Y. Chen, and P. W. Hsu, "Integrated dual planar inverted-F antenna with enhanced isolation," *IEEE Antennas Wireless Propag. Lett.*, Vol. 8, 963–965, 2009.
3. Wang, Y. and Z. Du, "A wideband printed dual-antenna with three neutralization lines for mobile terminals," *IEEE Trans. Antennas Propag.*, Vol. 62, No. 3, 1495–1500, 2014.
4. See, C. H., R. A. Abd-Alhameed, Z. Z. Abidin, N. J. McEwan, and P. S. Excell, "Wideband printed MIMO/diversity monopole antenna for WiFi/WiMAX applications," *IEEE Trans. Antennas Propag.*, Vol. 60, No. 4, 2028–2035, Apr. 2012.
5. Su, S.-W., C.-T. Lee, and F.-S. Chang, "Printed MIMO-antenna system using neutralization-line technique for wireless USB-dongle applications," *IEEE Trans. Antennas Propag.*, Vol. 60, No. 2, 456–463, Feb. 2012.
6. Lai, X. Z., Z. M. Xie, X. L. Cen, and Z. Y. Zheng, "A novel technique for broadband circular polarized PIFA and diversity PIFA systems," *Progress In Electromagnetics Research*, Vol. 142, 41–55, 2013.
7. Zuo, S., Y.-Z. Yin, Y. Zhang, W.-J. Wu, and J.-J. Xie, "Eigenmode decoupling for MIMO loop-antenna based on 180 coupler," *Progress In Electromagnetics Research Letter*, Vol. 26, 11–20, 2011.
8. Yeung, L. K. and Y. E. Wang, "Mode-based beamforming arrays for miniaturized platforms," *IEEE Trans. Microw. Theory Tech.*, Vol. 57, No. 1, 45–52, Jan. 2009.
9. Coetzee, J. C. and Y. Yu, "Port decoupling for small arrays by means of an eigenmode feed network," *IEEE Trans. Antennas Propag.*, Vol. 56, No. 6, 1587–1593, Jun. 2008.
10. Yang, F. and Y. Rahmat-Samii, "Microstrip antennas integrated with Electromagnetic Band-Gap (EBG) structures: A low mutual coupling design for array applications," *IEEE Trans. Antennas Propag.*, Vol. 51, No. 10, 2936–2946, Oct. 2003.
11. Li, Q., A. P. Feresidis, M. Mavridou, et al., "Miniaturized double-layer EBG structures for broadband mutual coupling reduction between UWB monopoles," *IEEE Trans. Antennas Propag.*, Vol. 63, No. 3, 1168–1171, 2015.
12. Li, L., B. Li, H. X. Liu, and C. H. Liang, "Locally resonant cavity cell model for electromagnetic band gap structures," *IEEE Trans. Antennas Propag.*, Vol. 54, No. 1, 90–100, Jan. 2006.
13. Suwailam, M., M. Boybay, and O. Ramahi, "Electromagnetic coupling reduction in high-profile monopole antennas using single-negative magnetic metamaterials for MIMO applications," *IEEE Trans. Antennas Propag.*, Vol. 58, No. 9, 2894–2902, Sep. 2010.

14. Habashi, A., J. Nourinia, and C. Gobadi, "Mutual coupling reduction between very closely spaced patch antennas using low-profile Folded Split-Ring Resonators (FSRRs)," *IEEE Antennas and Wireless Propagation Letters*, Vol. 10, 2011.
15. Qian, K.-W., L. Zhao, and K.-L. Wu, "An LTCC coupled resonator decoupling network for two antennas," *IEEE Trans. Antennas Propag.*, Vol. 63, No. 10, 3199–3207, Oct. 2015.
16. Zhao, L., K.-W. Qian, and K.-L. Wu, "A cascaded coupled resonator decoupling network for mitigating interference between two radios in adjacent frequency bands," *IEEE Trans. Microw. Theory Techn.*, Vol. 62, No. 11, 2680–2688, Nov. 2014.
17. Zhao, L. and K.-L. Wu, "A decoupling technique for four-element symmetric arrays with reactively loaded dummy elements," *IEEE Trans. Antennas Propag.*, Vol. 62, No. 8, 4416–4421, Aug. 2014.
18. Yeung, L. K. and K.-L. Wu, "A compact second-order LTCC band-pass filter with two finite transmission zeros," *IEEE Trans. Microw. Theory Techn.*, Vol. 51, No. 2, 337–341, 2003.
19. Zhao, L., L. K. Yeung, and K.-L. Wu, "A coupled resonator decoupling network for two-element compact antenna arrays in mobile terminals," *IEEE Trans. Antennas Propag.*, Vol. 62, No. 5, 2767–2776, May 2014.
20. Zhao, L. and K.-L. Wu, "A broadband coupled resonator decoupling network for a three-element compact array," *IEEE MTT-S Int. Microw. Symp. Dig.*, Jun. 2013.